Earth Surface Processes and Landforms
Earth Surf. Process. Landforms **24**, 413–422 (1999)

AEOLIAN MASS TRANSPORT NEAR THE SALTATION THRESHOLD

KELD R. RASMUSSEN[1]* AND MICHAEL SØRENSEN[2]
[1]*Department of Earth Sciences, University of Aarhus, Denmark*
[2]*Department of Theoretical Statistics, University of Copenhagen, Denmark*

Received 31 July 1998; Revised 23 October 1998; Accepted 23 October 1998

ABSTRACT

Aeolian mass transport was investigated in a desert field experiment where the wind speeds were near the saltation threshold. Bed transport was observed during 45 min runs even though the calculated values of bed shear stress using conventional laboratory equations for mass transport predicted that there should be no transport. We therefore investigated the possibility of predicting mass transport using quasi-instantaneous wind speeds, i.e. values derived at a time scale similar to that of the saltation process. Quasi-instantaneous wind speeds are able to predict mass transport associated with the stronger gusts. Predicted mass transport values compare fairly well with observation, but the accuracy of the prediction is very sensitive to correct estimation of the surface roughness and the saltation threshold for the particular sand bed. When these values differ by only 10 percent from the values that optimize the estimation, predicted mass transport can differ by up to ±50 per cent.

KEY WORDS: mass transport; near threshold; quasi-instantaneous wind; prediction

INTRODUCTION

Experiments conducted in laboratory wind tunnels are a primary source for information on aeolian grain mechanics. For instance, there exist far more data from laboratory experiments (e.g. Chepil and Milne, 1939; Bagnold, 1941; Kawamura, 1951; Zingg, 1953; Williams, 1964; Owen, 1964; Jones and Willetts, 1979; Greeley *et al.*, 1984; Iversen *et al.*, 1987; Rasmussen and Mikkelsen, 1991; Iversen and Rasmussen, 1994, 1999), on how grain movement is initiated by wind and how mass transport depends on wind strength than are available from similar observations in nature (Horikawa *et al.*, 1984; Jensen *et al.*, 1985; Hardisty and Whitehouse, 1988; Greeley *et al.*, 1996; Jackson and McCloskey, 1997). In the laboratory, wind direction and speed, turbulence intensity, sand supply and grain characteristics can be controlled by the investigator. Thus for a particular sand sample the static and dynamic thresholds of movement as well as the response of mass flux to bed shear stress can be related to the logarithmic wind speed profile above the bed (Bagnold, 1941).

In nature, the static and dynamic thresholds of movement, and the response of mass flux to the shear stress are difficult to investigate. Firstly, most aeolian transport takes place on curved or irregular surfaces where the constant-stress layer is very thin (Hunt *et al.*, 1988) and conventional measurement techniques using wind profiles recorded with cup anemometers are inadequate. Secondly, the range of turbulent eddies in nature is far wider than in the laboratory and hence the instantaneous stress at the bed varies more. Thus near the threshold of movement, long calm periods with wind speeds below the saltation threshold alternate with short intervals with strong turbulent eddies and sudden grain movement (Stout and Zobeck, 1997; Jackson, 1996; Jackson and McCloskey, 1997). In addition, turbulence results in short-term variations in the wind direction while synoptic changes cause longer-term shifts in the average wind direction and speed. Characterizing the

* Correspondence to: Dr K. R. Rasmussen, Department of Earth Sciences, University of Aarhus, Aarhus, Denmark. Email: geolkrr@aaw.dk
Contract/grant sponsor: Danish Natural Sciences Research Council

CCC 0197-9337/99/050413–10 $17.50

initiation of mass transport by using conventional average flow statistics must inevitably be inadequate, the more so since mass transport responds non-linearly to shear stress (Sørensen, 1997).

In order to study grain response to natural winds we have made a desert study of intermittent saltation where the flow was recorded at high frequency within the saltation layer together with total mass transport. Using a conventional equation relating mass flux to friction speed we will discuss how mass transport relates to the velocity observations and how sensitive the prediction will be to the choice of variables.

WIND FLOW AND MASS TRANSPORT

The discussion is limited to two-dimensional flow with the two components of the wind vector $V = (U, W)$. The U component (parallel to the x-axis) is in the direction of the mean wind so that $U = u + u'$, where u is the time-averaged quantity and u' is the fluctuation. W is the vertical component which has $w = 0$. The fluid shear stress τ_w at the bed is:

$$\tau_w = -\rho\overline{u'w'} \tag{1a}$$

where ρ is air density, while the friction speed u_* is conventionally defined as:

$$u_*^2 = \frac{\tau_w}{\rho} \tag{1b}$$

In the constant-flux layer near the surface the mean wind speed (u) at height z is given by the logarithmic wind law:

$$\frac{u(z)}{u_*} = \frac{1}{k}\ln\frac{z}{z_o} \tag{2}$$

where z_o is the roughness length and κ is von Kármán's constant. During saltation it is observed (e.g. Owen, 1964; Rasmussen *et al.*, 1996) that the roughness length increases moderately with increasing mass transport. Since we consider only mass transport in a small range of friction speeds just above the threshold we can neglect variations in z_o during the experiment. The roughness still increases abruptly, however, when saltation starts. Therefore, if we use Equation 2 to estimate u_* and z_o from wind data that represent average values over periods of 30 min to 1 h then such estimates will not pertain fully to saltation conditions.

On a quiescent sand bed initiation of grain movement into saltation requires grains to be entrained by the force of the wind itself (Anderson *et al.*, 1991). This occurs when the wind strength momentarily increases so that the bed shear stress locally exceeds the fluid threshold u_{*t} (for a discussion of the physics involved when a grain is plucked by the air stream see e.g. Anderson *et al.*, 1991). Once dislodgement of grains is enough to establish the cascade reaction (which leads to a fully developed saltation cloud) then grain transport is sustained by the collision of saltating grains with the bed, i.e. via splash (Willetts and Rice, 1986; Anderson *et al.*, 1991). We denote the time for the chain reaction to develop by Θ_s (the splash time scale), whereas we denote the period during which the boundary-layer flow after the splash adjusts to the excess friction created by the saltation cloud by Θ_a (the boundary-layer adjustment time scale). Both Θ_s and Θ_a are small, Θ_s being probably of the order of 1 s or less (McEwan and Willetts, 1991; Jackson and McCloskey, 1997) and Θ_a of the order of 5 to 10 s (McEwan and Willetts, 1991; Butterfield, 1991). Therefore, the characteristics of the saltation cloud are closely linked to the momentary state of the wind near the bed (McEwan and Willetts, 1991; Jackson, 1996).

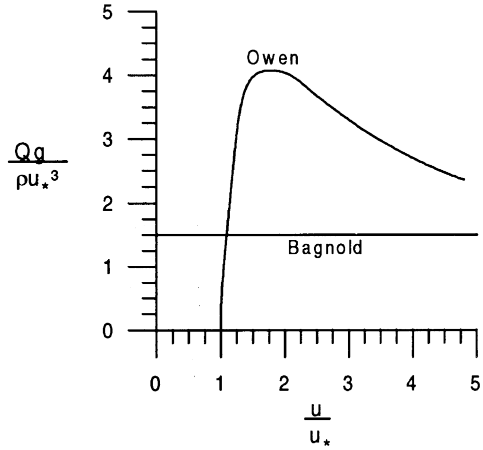

Figure 1. Normalized dimensionless transport rate ($Qg/\rho u_*^3$) plotted versus normalized friction speed (u/u_*) for the equations proposed by Bagnold (1941) and Owen (1964)

For the steady saltation process Owen (1964) proposed that the normalized dimensionless transport rate q can be expressed as:

$$q = \frac{Qg}{\rho u_*^3} = \left(C + \frac{U_F}{3u_{*t}}\right)\left(1 - \left(\frac{u_{*t}}{u_*}\right)^2\right) \tag{3}$$

where C is a constant (= 0·25), U_F is the terminal velocity, g is gravity, and Q is the net transport per second per unit width perpendicular to the direction of the wind. Several equations relating q and u_* have been proposed, but Iversen and Rasmussen (1998) find that Equation 3 fits most experimental data quite well. However, they use $C = 1{\cdot}0$ which will be used in the following. One should notice that q increases rapidly just above the threshold and then reaches a maximum (overshoot) from where it gradually decreases (Figure 1). For comparison, the dimensionless form of the transport equation by Bagnold (1941) is also depicted in Figure 1 (for details see e.g. Rasmussen and Mikkelsen, 1991). Thus while q in general is sensitive to any variations in u_*, Figure 1 shows clearly that near the threshold q is particularly sensitive to such variations.

Inserting u_* in Equation 3 (or a similar equation) in order to predict aeolian mass transport in a turbulent flow must inevitably result in biased estimation. However, one might expect that Equation 3 will be valid if we can divide the flow record into short quasi-stationary segments, i.e. so that each segment represents an 'effective shear velocity' u_{*s} over a time interval of length Θ_a. When rearranging Equation 2 we find:

$$\bar{u_{*s}} = \frac{\kappa \bar{u}_s}{\ln\left[\frac{z_s}{z_o}\right]} \tag{4}$$

in which u_{*s} relates to the average speed (u_s) at height z over time intervals of length Θ_a. During transport, i.e. when $u_{*s} > u_{*t}$, we can thus rearrange Equation 3, insert u_{*s} instead of u_* and find the quasi-momentary transport rate:

$$Q_s = \frac{\rho}{g}\overline{u_{*s}}^3\left(1 + \frac{U_F}{3u_{*t}}\right)\left(1 - \left(\frac{u_{*t}}{\overline{u_{*s}}}\right)^2\right) \tag{5}$$

For longer periods we propose that the total transport can be obtained as the sum of momentary contributions during intervals in which $u_{*s} > u_{*t}$.

Figure 2. The test area at the Jornada Experimental Range, New Mexico. The mast for the velocity measurements is in the centre. Suction tubes to the isokinetic sensor and box with valves and settling chambers are placed on the right-hand side of the mast

FIELD SITE AND METHODS

The field work for this study was conducted at the Jornada Experimental Range near Las Cruses, New Mexico. The vegetation had been removed on the test area (Figure 2) prior to the experiment. Under the influence of the predominantly south-southwest winds the topsoil has drifted to the northeastern end of the test area where it forms a shallow sand drift (low dune). The drift is primarily composed of medium sand with a median grain size of about 320 μm and forms a virtually flat, loose sand bed during the experiment.

Wind data were sampled on a 1·8 m portable mast (Figure 3) using a DANTEC 55R01 split-fibre sensor connected to a DANTEC CTA-Streamline system. The sensor is made of a ceramic rod, 3 mm long and 200 μm thick, with a Pt-coating, but only the central 1·25 mm of the platinum is sensitive to cooling. The upper and lower halves of the coating are separated electrically and their responses (E1 and E2) to cooling depends on the speed (U) as well as the pitch angle (ϕ) of the incoming flow relative to the probe axis. Thus $U \propto E_1 + E_2$ while $\phi \propto E_1 - E_2$. (Actually, ϕ depends slightly on the speed, too, but this dependence is included in the conversion routine (Rasmussen, 1997).) Since the split-fibre has a near-cosine response for small yaw-angles we can calculate the average components u and w for each run as well as τ_w using Equation 1a.

The sensor was placed as close to the bed as possible, typically at height z between 5 cm and 15 cm ($\pm$1 mm), and pointed into the wind with the fibre perpendicular to the mean wind direction. The aerodynamic roughness length z_o of a sand surface is small –typically less than 1 mm, even during moderate transport (Rasmussen *et al.*, 1996). The height z was chosen so that $z/z_o \geq 100$ and thus our physical measurements were made well above the roughness layer (Garratt, 1992). During the day, the mean wind direction was constantly assessed from a simple wind vane and small adjustments were made to the orientation of the sensor between the different runs. It was observed that during periods with moderate to high wind speeds the changes in the wind direction were small whereas in the intervening calm periods large excursions from the average direction were observed. Quasi-continuous wind measurements were recorded concurrent with mass transport measurements (see below) for approximately 45 min at a sampling rate of 20 Hz (2 s were used for writing data to disk after each block of 8192 data, i.e. at about 7 min intervals).

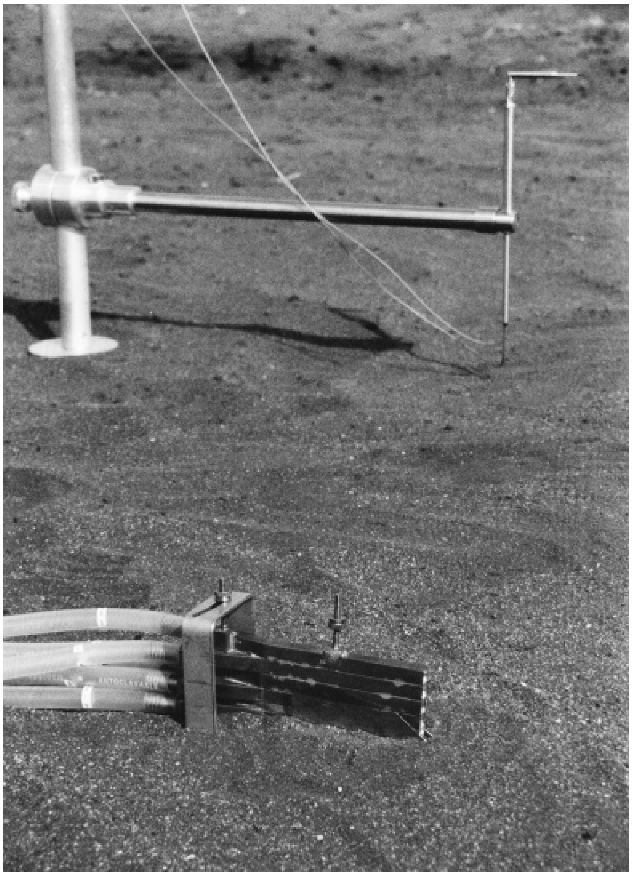

Figure 3. The split-fibre sensor and the isokinetic trap placed at the test area. The sensor protrudes horizontally from the L-shaped support at the end of the 0·5 m long arm on the mast. The isokinetic trap is placed on the bed and the front horns are visible at the lowest sample tube. The suction and settling chambers are behind the mast outside the field of view

On a sand bed with saltation the majority of the mass transport takes place within a few centimetres above the bed. Unfortunately, flow here is sensitive to distortion by a trap (Rasmussen and Mikkelsen, 1998). Therefore, we measured transport between the surface and a height of 45 mm using a modified version of an 8 mm wide isokinetic laboratory trap (for details see Rasmussen and Mikkelsen, 1998). This consists of six brass tubes, each connected to a settling chamber and a valve that controls the air flow through the trap to a common suction chamber. The upper four tubes are 9 mm high, but the lower two are only 4·5 mm so that the ventilation through each tube can be adjusted reasonably isokinetically to the speed of the surrounding air.

During experiments the lowest tube was placed directly on the bed and the position of the trap adjusted carefully in order to keep the bottom of the lowest compartment flush with the local surface. All tubes were sharpened at the leading edge so that the apertures facing the flow had well defined cross-sections. Because of turbulence, the wind direction varied during field operation and, therefore, small horns were fitted along the sides of the lowest chamber in order to prevent cross-winds from scouring beneath the front of the trap. Before each experiment (but during transport), adjustment of the valves for isokinetic operation was performed. Since the wind is turbulent, we cannot obtain fully isokinetic conditions, but laboratory simulations show that the efficiency of sample tubes is not strongly affected by moderate deficiencies in the ventilation of the trap (Rasmussen and Mikkelsen, 1998).

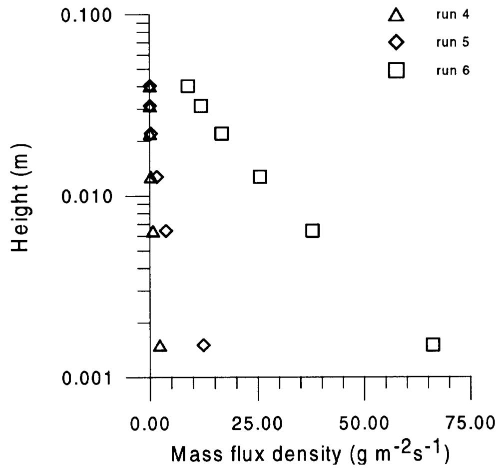

Figure 4. Flux density data during three runs. Sample tube height is calculated as the geometric mean height of the top and bottom of each tube.

RESULTS

Concurrent data for total mass transport and near-bed wind speeds were recorded during approximately a week during which sediment transport took place for a total of approximately 12 h. Twelve data sets were obtained with each run lasting about 45 min. Around 15 min was required between successive runs for backup of data, preparations, and the maintenance of equipment.

Mass transport

The transport rates were small, ranging from about 5×10^{-5} kg m^{-1} s^{-1} to a little over 10^{-3} kg m^{-1} s^{-1} as calculated over the entire length of each run. However, continuous transport was not observed during the full length of any run. Despite the small amounts of trapped material, the data are consistent with respect to the relative catch of the sample tubes (Figure 4). Data are given for three different runs spanning almost the entire range of transport rates.

The maximum transport was measured in run 6 and in this run the plot of flux density against log height is very close to a straight line (exponential behaviour). The lower transport rates in run 4 and run 5 decrease more slowly with height, and there are signs of a further decrease in the flux gradient near the top, i.e. the exponential behaviour is less perfect. Exponential profiles have also been observed in the wind tunnel by Williams (1964) except just above the surface and by Rasmussen and Mikkelsen (1998), but their data were recorded only at transport rates higher than those encountered in the present experiment.

Since our trap only measures transport near the bed, the mass of grains that is being transported above the trap is estimated by extending each flux density profile to the intersection with the y-axis. The calculated corrections vary in the range of 5 to 15 per cent.

Wind data

Values of u_* were calculated for each of the 12 runs using Equations 1a and 1b. The results are depicted in Figure 5. Friction speeds vary considerably, i.e. from 0·10 m s^{-1} to about 0·22 m s^{-1}, but all values are very small. None of the values, in fact, exceeds the static threshold ($u_{*\mathrm{t,stat}}$ 0·30 m s^{-1}) which was assessed in the wind tunnel using a tray, 4 m long and 0·4 m wide, covered with sample material. Although the laboratory estimation is rather crude there is no doubt that the static threshold far exceeds the u_* values that were measured in all 12 field runs. This clearly indicates how inadequate the traditional shear stress value is in estimating mass transport in the field.

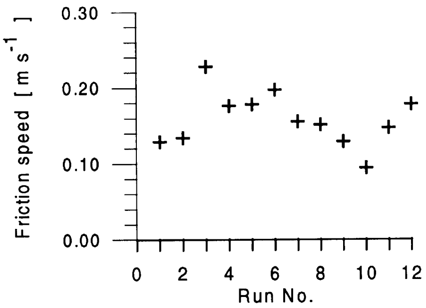

Figure 5. Friction speeds for the 12 runs at the Jornada Experimental Range

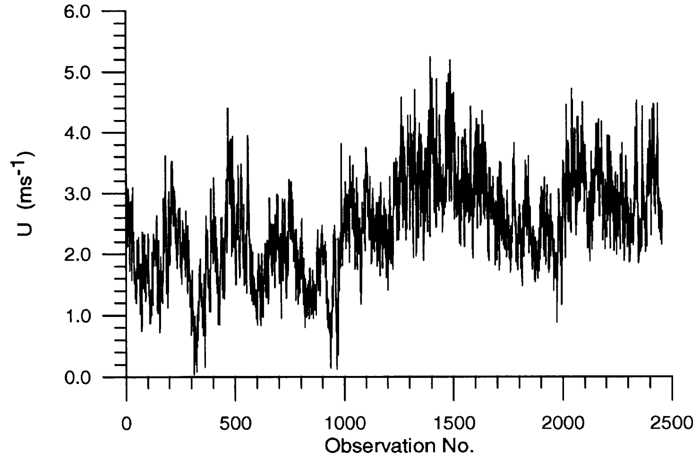

Figure 6. One-second low-pass-filtered data for the *u* component during run 6

Calculation of mass transport

The influence of eddies of timescale less than Θ_s in the U-signals was removed with a 1 s moving-average filter. The resulting series for run 6 is shown in Figure 6. (Series with 2 and 3 s moving-average filters were also constructed, but since they deviate little from Figure 6 they are not presented here.) As can be seen, the wind speed varied from almost zero to more than 5 m s^{-1} during the 40 min period. In particular one should note the period of strong winds between samples 1200 and 1500.

The values of z_o and u_{*t} are difficult to assess precisely from independent field observation. Therefore, we decided to calibrate the two parameters by minimizing the deviations between observed and predicted mass transport. During our calculations we used $u_{*t,dyn} = 0{\cdot}8\ u_{*t,stat}$ (Bagnold, 1941).

With initial values of z_o and $u_{*t,stat}$ (taken from the wind tunnel check) we rearrange Equation 4 and calculate the speed ($u_{t,\ stat}$) at height z which corresponds to $u_{*t,stat}$. Likewise we find the speed $u_{t,\ dyn}$ that corresponds to $u_{*t,dyn}$. In order to assess the momentary contributions from the wind to sediment transport we then start at the first measurement in each low-pass filtered series and search until the speed exceeds $u_{t,\ stat}$. From there we calculate the average speed (u_s) during the next 5 s. If $u_s > u_{t,\ dyn}$ we calculate the contribution to mass transport according to Equation 5, and continue the search after the 5 s interval. If $u_s < u_{t,\ dyn}$ we discard the value and resume the procedure at the next value at which the speed originally exceeded $u_{t,\ stat}$. Thus from each series we sum momentary transport contributions to obtain the total transport during the particular run. By a search procedure, optimal values for z_o and $u_{*t,stat}$ are obtained, i.e. the values that predict the average transport that was measured during the field experiment.

From the calibration we find $z_o = 0{\cdot}001$ m while $u_{*t,stat} = 0{\cdot}31$ m s^{-1}, and with these values the predicted mass transport is plotted versus measured transport in Figure 7. There is quite some scatter in the data, but

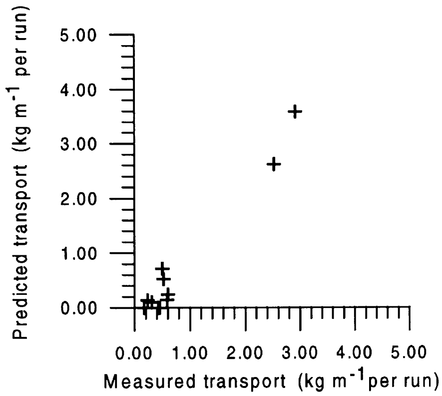

Figure 7. Comparison between predicted and measured mass transport during each of the 12 runs

except for run 5, in which the transport is somewhat underestimated, the prediction seems to be reasonable, especially in view of the fact that the wind speed is close to the saltation threshold.

The calculation also enables us to estimate the duration of transport during each run (Figure 8a). The figure shows that in two-thirds of the runs transport is predicted during only 5 per cent or less of the time. The maximum duration is estimated to about 15 per cent. We define a transport event as an interval with transport preceded and followed by intervals without transport. The number of transport events that the model predicts is shown in Figure 8b. In runs with very low transport there are few events; however, as the transport intensity increases the number of events becomes high. The calculations thus support our visual observations that the saltation process was strongly intermittent even during the run with the most intense transport.

DISCUSSION

The value of 0·31 m s^{-1} that we find for $u_{*t,stat}$ is very close to the value that was assessed in the wind tunnel. The value for z_o on the other hand is rather large, at least compared to the values that one finds in wind tunnels (Rasmussen *et al.*, 1996). However, high values of z_o were also recorded in a previous field experiment at a beach (Rasmussen *et al.*, 1985). Anyhow, our data indicated that if the z_o value were significantly lowered in the calculations then we would predict no transport at all during the runs with the lowest wind speeds (and mass transport). So, tentatively, we think that the small irregularities on the natural surface makes this rougher than on similar bed materials in the wind tunnel.

As a further check of the prediction calculation we investigated how sensitive our predictions are to small perturbations in the parameters. First we repeated the calculation using 10 and 15 s averaging intervals instead of 5 s. As can be expected from this simple averaging process, the transport rates decrease which in turn affects the estimates of z_o and u_{*t}. If, on the other hand, the z_o and $u_{*t,stat}$ values from the 5 s are retained during the prediction with the 10 s averaging period, then transport values amount to 85–90 per cent of that based on the 5 s period. This suggests that the calculation will depend only moderately on the choice of averaging period.

Secondly, we checked how sensitive prediction of the total transport during all 12 runs (Q_s) is to variations in z_o and $u_{*t,stat}$. The total transport that we predict using $z_o = 0{\cdot}001$ m and $u_{*t,stat} = 0{\cdot}31$ m s^{-1} we denote by Q_{so}. Now we change first z_o and then $u_{*t,stat}$ by ± 10 per cent, respectively, and repeat the prediction using the new values (Table I). From Table I it is evident that the calculations are very sensitive to the choice of any of the two parameters. Thus, when these values differ by only 10 per cent from the values that optimize the estimation, predicted mass transport can differ by up to ± 50 per cent. The strong sensitivity, on the other hand, indicates that estimation is possible using the proposed method.

The calculations are performed for a limited number of data in the range of friction speeds where calculations, at least on a relative scale, are probably very sensitive to any perturbation in the parameters. It is

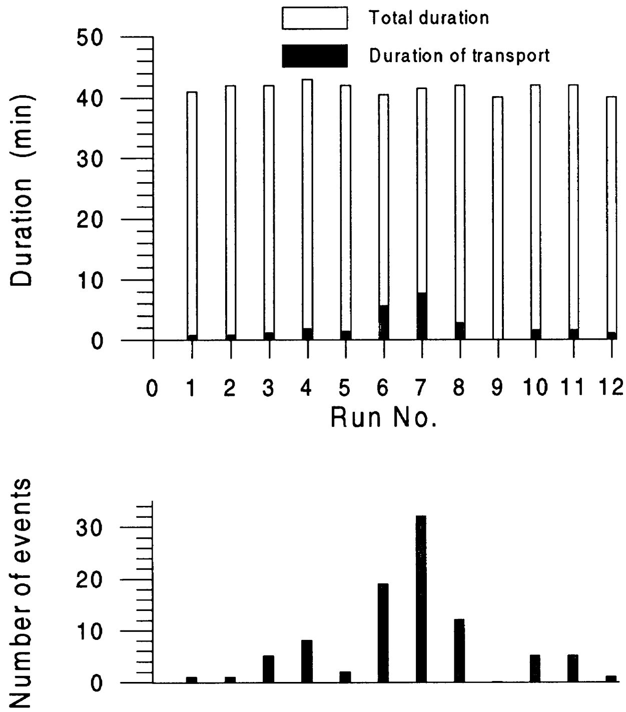

Figure 8. (a) Total duration of transport and (b) the number of transport 'events' in each run.

Table I. Sensitivity of the mass prediction to parameter changes

Parameter	$u_{*t,stat}$	$u_{*t,stat}$	Z_o	Z_o
Deviation ()	−10	10	−10	10
Q_s/Q_{so}	1·59	0·44	0·60	1·71

therefore necessary to check the prediction errors of similar calculations at higher friction speeds where the prediction will be less influenced by the exact value of $u_{*t,stat}$. Nevertheless, our results clearly indicate that although the use of aeolian traps in the field may seem extremely difficult to operate, there is no easy way of substituting transport measurements with predictions using wind data, although it is obviously far less complicated to measure air flow than sand mass flux in the field.

On the other hand, since mass transport is sensitive to changes in wind speed, such studies reveal important information about grain dynamics and the interaction between wind flow and mass transport. Since relatively little is known of how mass flux responds to turbulence, it seems particularly important that we measure simultaneously and at short time resolution wind flow as well as mass transport.

CONCLUSIONS

The field investigation which was carried out at and slightly above the saltation threshold supports laboratory findings of a strong increase in mass transport with friction speed (wind speed) as predicted by Owen (1964). Likewise, turbulent fluctuations will dominate the transport process near threshold and create strong intermittency in saltation. When predicting mass transport using near-bed wind data our simple model indicates that transport is very sensitive to variations (changes) in surface roughness and saltation threshold; such changes could result, for instance, from armouring of the surface during saltation. Finally, we find that

currently there is much uncertainty when predicting mass transport in detail without thorough calibration of the local values of surface roughness and threshold friction speed.

ACKNOWLEDGEMENTS

The Danish Natural Sciences Research Council has supported this investigation through a grant for travel and instruments. The USDA/ARS, Jornada Experimental Range has kindly permitted us to perform the field investigation on their research grounds, and we particularly thank Dr Kris Havstad for kind assistance. Finally, we thank Gary Beardmore, Planetary Geology Group, Arizona State University, Tempe, for valuable technical assistance.

REFERENCES

Anderson, R. S., Sørensen, M. and Willetts, B. B. 1991. 'A review of recent progress in our understanding of aeolian sediment transport', in Barndorff-Nielsen, O. E. and Willetts, B. B. (Eds), Aeolian Grain Transport 1: Mechanics, *Acta Mechanica*, Suppl. 1, 1–20.

Bagnold, R. A. 1941. The physics of blown sand and desert dunes. Methuen, London, 265 pp.

Butterfield, G. R. 1991. 'Grain transport rates in steady and unsteady turbulent airflows', in Barndorff-Nielsen, O. E. and Willetts, B. B. (Eds), Aeolian Grain Transport 1: Mechanics, *Acta Mechanica* Suppl. 1, 97–122.

Chepil, W. S. and Milne, R. A. 1939. 'Comparative study of soil drifting in the field and in a wind tunnel', *Scientific Agriculture*, **19**, 149–257.

Garratt, J. R. 1992. The Atmospheric Boundary Layer, Cambridge University Press, New York.

Greeley, R., Blumberg, D. G. and Williams, S. H. 1996. 'Field measurement of the flux and speed of wind-blown sand', *Sedimentology*, **43**, 41–52.

Greeley, R., Iversen, J. D., Leach, R., Marshall, J. R., White, B. and Williams, S. 1984. 'Windblown sand on Venus: Preliminary results of laboratory simulations', *Icarus*, **57**, 112–124.

Hardisty, J. and Whitehouse, R. J. S. 1988. 'Evidence for a new sand transport process from experiments on Saharan dunes', *Nature*, **332**(7), 532–534.

Hunt, J. C. R., Leibovich, S. and Richards, K. J. 1988. 'Turbulent shear flows over low hills', *Quarterly Journal of the Royal Meteorological Society*, **114**, 1435–1470.

Iversen, J. D., Greeley, R. Marshall, J. R. and Pollack, J. B. 1987. 'Aeolian saltation threshold: the effect of density ratio', *Sedimentology*, **34**, 699–706.

Iversen, J. D. and Rasmussen, K. R. 1994. 'The effect of surface slope on saltation threshold', *Sedimentology*, **41**, 721–728.

Iversen, J. D. and Rasmussen, K. R. 1999. 'The effect of wind speed and bed slope on sand transport', *Sedimentology*, (submitted).

Jones, J. R. and Willetts, B. B. 1979. 'Errors in measuring aeolian flow by means of an adjustable trap', *Sedimentology*, **26**, 463–468.

Kawamura, R. 1951. Study on sand movement by wind, Reports of Physical Sciences Research Institute of Tokyo University, Vol. 5, No. 3–4, 95–112. (translated from Japanese by National Aeronautic and Space Administration (NASA), Washington D.C., 1972).

McEwan, I. K. and Willetts, B. B. 1991. 'Numerical model of the saltation cloud', in Barndorff-Nielsen, O. E. and Willetts, B. B., (Eds), Aeolian Grain Transport 1: Mechanics, *Acta Mechanica* Suppl. 1, 53–66.

Owen, P. R. 1964. 'Saltation of uniform grains in air', *Journal of Fluid Mechanics*, **20**, 225–242.

Rasmussen, K. R. 1997. Application of the Dantec 55 R01 split-fibre sensor for studies of wind-blown sand, unpublished technical report, Department of Earth Sciences, University of Aarhus, Denmark, 12 pp.

Rasmussen, K. R. and Iversen, J. D. 1996. 'Grain dynamics and wind-flow in a variable slope wind tunnel', Proceedings of The International Conference on Desert Development in the Arab Gulf Countries, Kuwait, 23–26 March 1996.

Rasmussen, K. R. and Mikkelsen, H. E. 1991. 'Wind tunnel observations of aeolian transport rates', in Barndorff-Nielsen, O. E. and Willetts, B. B., (Eds), Aeolian Grain Transport: 1 Mechanics, *Acta Mechanica* Suppl. 1, 135–144.

Rasmussen, K. R. and Mikkelsen, H. E. 1998. 'On the efficiency of vertical array aeolian field traps', *Sedimentology*, **45**, 789–800.

Rasmussen, K. R., Sørensen, M., Willetts, B. B. 1985. 'Measurement of saltation and wind strength on beaches', in Barndorff-Nielsen, O. E. and Willetts, B. B., (Eds) Proceedings of International Workshop on the Physics of Blown Sand, Department of Theoretical Statistics, Aarhus University, Denmark, Vol. **2**, 301–325.

Rasmussen, K. R., Iversen, J. D. and Rautaheimo, P. 1996. 'Saltation and wind-flow interaction in a variable slope wind tunnel'. *Geomorphology*, **17**, 19–28.

Sørensen, M. 1997. 'On the effect of time variability of the wind on rates of aeolian sand transport,' *Aarhus Geoscience*, **7**, 73–77, (Department of Earth Sciences, University of Aarhus).

Stout, J. E. and Zobeck, T. M. 1997. 'Intermittent saltation', *Sedimentology* **44**, 959–970.

Willetts, B. B. and Rice, M. A. 1986. 'Collision in aeolian transport: the saltation/creep link', in Nickling, W. G. (Ed.), Aeolian Geomorphology, Allen and Unwin, Boston, 1–17.

Williams, G. 1964. 'Some aspects of aeolian saltation load', *Sedimentology*, **3**, 257–287.

Zingg, A. W. 1953. 'Wind tunnel studies of movement of sedimentary material', Proceedings of the 5th Hydraulic Conference, Bulletin 34, 111–134.

